

Synthesis, Crystal Structure and DNA-Binding Properties of a Cadmium(II) Complex with 2,6-Bis(*N*-methylbenzimidazol-2-yl)pyridine

Huilu Wu, Xingcai Huang, Jingkun Yuan, Fan Kou, Fei Jia, Bin Liu, and Ying Bai

School of Chemical and Biological Engineering, Lanzhou Jiaotong University, Lanzhou 730070, P. R. China

Reprint requests to Dr. Huilu Wu. E-mail: wuhuilu@163.com

Z. Naturforsch. **2011**, *66b*, 1049 – 1055; received July 6, 2011

A new complex of Cd(II) picrate (pic) based on the ligand 2,6-bis(*N*-methylbenzimidazol-2-yl)pyridine (mbbp) has been synthesized and characterized by elemental analysis, electrical conductivity, ^1H NMR, IR and UV/Vis spectral measurements. The crystal structure of the Cd(II) complex, $[\text{Cd}(\text{mbbp})_2](\text{pic})_2$, has been determined by single-crystal X-ray diffraction. The Cd(II) cation is bonded to two mbbp ligands through six nitrogen atoms, resulting in a distorted octahedral geometry. Interaction of the complex with DNA was investigated by spectrophotometric methods and viscosity measurements. The experimental results suggest that the Cd(II) complex binds to DNA in an intercalation mode.

Key words: 2,6-Bis(*N*-methylbenzimidazol-2-yl)pyridine, Cd(II) Complex, Crystal Structure, DNA-Binding Properties

Introduction

Transition metal complexes are used to bind and react at specific sequences of DNA for finding novel chemotherapeutics, probing DNA and developing highly sensitive diagnostic agents [1, 2]. Therefore, an understanding of how these small molecules bind to DNA will be potentially useful for the design of new drugs, structural and diagnostic probes and reactive agents which can recognize specific sites or conformations of DNA [3–5].

Because of the good biological activities of 2,6-bis(2-benzimidazolyl)pyridine (bbp) and its transition metal complexes [6–11] the ligand 2,6-bis(*N*-methylbenzimidazol-2-yl)pyridine (mbbp) has also been studied focusing on the interactions of transition metal complexes with DNA. In our previous studies [12, 13], the interactions of the Mn(II) and Ni(II) picrate complexes based on the ligand bbp with DNA were been studied. Herein we give a full account on the synthesis, crystal structure and DNA-binding properties of the Cd(II) picrate complex with 2,6-bis(*N*-methylbenzimidazol-2-yl)pyridine (mbbp).

Experimental Section

Materials and physical measurements

Ethidium bromide (EB) and calf thymus DNA (CT-DNA) were obtained from Sigma Chemicals Co. (USA). Tris-HCl

buffer solution was prepared using bidistilled water. Other reagents and solvents were reagent grade obtained from commercial sources and used without further purification. The solution of CT-DNA gave a ratio of UV absorbance at 260 and 280 nm, A_{260}/A_{280} , of 1.8–1.9, indicating that the DNA was sufficiently free of protein [14]. The stock solution of the complex was dissolved in DMF at the concentration 1×10^{-3} M. The stock solution of DNA (2.5×10^{-3} M) was prepared in 5 mM Tris-HCl/50 mM NaCl buffer (pH = 7.2, stored at 4 °C and used within 4 d). The DNA concentration was determined by measuring the UV absorption at 260 nm, taking the molar absorption coefficient (ϵ_{260}) of CT-DNA as $6600 \text{ M}^{-1} \text{ cm}^{-1}$ [15].

Elemental analyses were performed on a Carlo Erba 1106 elemental analyzer. IR spectra were recorded on a Bruker FT-IR Vertex 70 spectrometer in the range $4000\text{--}400 \text{ cm}^{-1}$ using KBr pellets. Electrolytic conductance measurements were made with a DDS-11A type conductivity bridge using a 10^{-3} M^{-1} solution in DMF at r.t. The ^1H NMR spectra were obtained with a Mercury plus 400 MHz NMR spectrometer with TMS as internal standard and CDCl_3 as solvent.

Electronic absorption spectra were taken on a Lab Tech UV Bluestar plus UV/Vis spectrophotometer. Using the electronic absorption spectral method, the relative binding of the complex to CT-DNA was studied in 5 mM Tris-HCl/NaCl buffer (pH = 7.2). The sample solution was scanned in the range 200–500 nm.

Fluorescence spectra were recorded on a 970CRT spectrofluorophotometer. While gradually adding a certain

amount of DMF solution of the complex step by step to the EB-DNA solution in Tris-HCl buffer at 25 °C, the emission intensity at 520 nm was recorded. The sample solution was scanned in the range 550–750 nm.

Viscosity experiments were conducted on an Ubbelohde viscosimeter, immersed in a thermostated water bath maintained at 25.0 ± 0.1 °C. DNA samples approximately 200 bp in an average length were prepared by sonication in order to minimize complexities arising from DNA flexibility [16]. Titrations were performed for the compounds ($1 - 10$ μ M), and the complex was introduced into the CT-DNA solution (50 μ M) present in the viscometer. Data are presented as $(\eta - \eta_0)^{1/3}$ versus the ratio of the concentration of the compound to CT-DNA, where η is the viscosity of CT-DNA in the presence of the complex, and η_0 is the viscosity of CT-DNA alone. Viscosity values were calculated from the observed flow time of CT-DNA-containing solutions corrected for the flow time of the buffer alone (t_0), $\eta = (t - t_0)/t_0$ [17].

Preparation of 2,6-bis(*N*-methylbenzimidazol-2-yl)pyridine (*mbbp*) and its cadmium(II) picrate complex

2,6-Bis(*N*-methylbenzimidazol-2-yl)pyridine (*mbbp*)

The ligand 2,6-bis(2-benzimidazolyl)pyridine was synthesized according to the procedure reported by Addison [18]. 2,6-Bis(2-benzimidazolyl)pyridine (3.11 g, 0.01 mol) in tetrahydrofuran (THF) (100 mL) was slowly added to potassium (0.77 g, 0.02 mol) under a nitrogen atmosphere. The mixture was stirred and heated under reflux for one hour until the potassium disappeared. The mixture was added to water, the precipitate was filtered and recrystallized from methanol, and yellow crystals were obtained. Yield 58 %, M. p. 194–196 °C. – IR (KBr, pellet, cm^{-1}): $\nu = 3060\text{m}$ ($\nu_{\text{C-H}}$), 1591m ($\nu_{\text{C=C}}$), 1568s ($\nu_{\text{C=N}}$), 1483w ($\nu_{\text{C=N}}$), 1438s , 1419m , 1396w , 1328s , 1288w ($\nu_{\text{C-N}}$), 1247m , 1197m , 1149m , 827s , 742s ($\delta_{\text{Ph(C-H)}}$). – ^1H NMR (400 MHz, CDCl_3 , 298 K): δ (ppm) = 8.42 (d, 2H, $J = 8.01$ Hz, Py-H), 8.06 (t, 1H, $J = 7.87$ Hz, Py-H), 7.88 (d, 2H, $J = 7.82$, Ph-H), 7.44 (d, 2H, $J = 7.56$, Ph-H), 7.38 (m, 4H, Ph-H), 4.24 (s, 6H, NCH_3). – UV/Vis (DMF): $\lambda = 306$, 388 nm. – Λ_{M} (DMF, 297 K): 5.0 $\text{S cm}^2 \text{mol}^{-1}$.

[Cd(*mbbp*)₂](pic)₂

To a stirred solution of 2,6-bis(*N*-methylbenzimidazol-2-yl)pyridine (0.1358 g, 0.40 mmol) in hot MeOH (10 mL) was added Cd(pic)₂ (0.1137 g, 0.20 mmol) dissolved in MeOH (5 mL). Owing to the formation of the [Cd(*mbbp*)₂]²⁺ complex, a pale-yellow precipitate was generated immediately. The sediment was filtered off, washed with MeOH and absolute Et₂O, and dried *in vacuo*. The dried precipitate was dissolved in DMF to give a yellow solution, and yellow crystals suitable for X-ray diffraction studies were obtained by vapor

Table 1. Crystal data and structure refinement for [Cd(*mbbp*)₂](pic)₂.

Complex	[Cd(<i>mbbp</i>) ₂](pic) ₂
Molecular formula	C ₅₄ H ₃₈ Cd N ₁₆ O ₁₄
Molecular weight, g mol^{-1}	1247.41
Color, habit	yellow, block
Crystal size, mm^3	$0.32 \times 0.24 \times 0.15$
Crystal system	monoclinic
Space group	<i>C</i> 2/ <i>c</i>
<i>a</i> , Å	22.007(4)
<i>b</i> , Å	17.019(3)
<i>c</i> , Å	13.891(3)
β , deg	104.88(3)
<i>V</i> , Å ³	5028.2(17)
<i>Z</i>	4
<i>T</i> , K	153(2)
<i>D</i> _{calcd} , g cm^{-3}	1.65
<i>F</i> (000), e	2536
μ (MoK α), mm^{-1}	0.5
θ range for data collection, deg	$3.03 - 27.48$
<i>hkl</i> range	$-27 \leq h \leq 28$, $-20 \leq k \leq 22$, $-18 \leq l \leq 18$
Reflections collected	24335
Independent reflections / <i>R</i> _{int}	5745 / 0.0182
Data / restraints / parameters	5745 / 2 / 386
Final <i>R</i> ₁ / <i>wR</i> ₂ indices [$I \geq 2\sigma(I)$] ^a	0.0226 / 0.0589
<i>R</i> ₁ / <i>wR</i> ₂ indices (all data) ^a	0.0246 / 0.0599
Goodness-of-fit (<i>F</i> ²) ^b	1.089
Largest diff. peak / hole, e Å^{-3}	0.53 / −0.48

^a $R_1 = \Sigma ||F_o| - |F_c|| / \Sigma |F_o|$, $wR_2 = [\Sigma w(F_o^2 - F_c^2)^2 / \Sigma w(F_o^2)^2]^{1/2}$, $w = [\sigma^2(F_o^2) + (0.0264P)^2 + 6.4911P]^{-1}$, where $P = (\text{Max}(F_o^2, 0) + 2F_c^2)/3$; ^b GoF = $[\Sigma w(F_o^2 - F_c^2)^2 / (n_{\text{obs}} - n_{\text{param}})]^{1/2}$.

diffusion of ether into the DMF solution after several days at r. t. Yield: 0.1321 g, 53 %. Analysis for C₅₄H₃₈N₁₆O₁₄Cd (1247.41): calcd. C 52.00, H 3.07, N 17.97; found C 52.01, H 3.11, N 17.95. – IR (KBr, pellet, cm^{-1}): $\nu = 1631\text{s}$, 1610s ($\nu_{\text{C=C}}$), 1568m ($\nu_{\text{C=N}}$), 1527w , 1473s ($\nu_{\text{C=N}}$), 1436w , 1420w , 1361m , 1330s , 1311s , 1263s ($\nu_{\text{C-N}}$), 1163m , 821w , 740s ($\delta_{\text{Ph(C-H)}}$). – UV/Vis (DMF): $\lambda = 298$, 363, 398 nm. – Λ_{M} (DMF, 297 K): 83.1 $\text{S cm}^2 \text{mol}^{-1}$.

X-Ray structure determination of [Cd(*mbbp*)₂](pic)₂

A suitable single crystal was mounted on a glass fiber, and the intensity data were collected on a Rigaku R-axis Spider diffractometer with graphite-monochromatized MoK α radiation ($\lambda = 0.71073$ Å) at 153 K. Data reduction and cell refinement were performed using RAPID-AUTO programs [19]. The absorption correction was carried out by the empirical method. The structure was solved by Direct Methods and refined by full-matrix least-squares methods against *F*² of all data using the SHELXTL software [20]. All H atoms were found in difference electron maps and were subsequently refined in a riding model approximation with C–H distances ranging from 0.95 to 0.98 Å and $U_{\text{iso}}(\text{H}) = 1.2$ or $1.5 U_{\text{eq}}(\text{C})$.

The H atoms bonded to N atoms were refined independently with the distance constraint of N–H = 0.88 Å. The atoms of one DMF solvent molecule are disordered over two coplanar orientations with equal occupancy. A summary of parameters for the data collection and the refinement is given in Table 1.

CCDC 830372 contains the supplementary crystallographic data for this paper. These data can be obtained free of charge from The Cambridge Crystallographic Data Centre via http://www.ccdc.cam.ac.uk/data_request/cif.

Results and Discussion

The ligand mbbp and the Cd(II) complex are remarkably soluble in polar aprotic solvents such as DMF, DMSO and MeCN, and also soluble in ethanol, methanol, ethyl acetate, and chloroform, but insoluble in water, Et₂O and petroleum ether. The molar conductivities in DMF solution indicate that mbbp is a nonelectrolyte, and the Cd(II) complex is a 1 : 2 electrolyte [21].

IR and electronic spectra

The IR spectral of the free ligand and the Cd(II) complex have been recorded and assigned to characterize the structures. The free ligand mbbp shows characteristic absorption bands of the benzimidazole pyridine group at 1591, 1568, 1483, and 1288 cm^{−1} assigned to $\nu_{C=C}$, $\nu_{C=N}$ and ν_{C-N} , respectively [22,23]. For free mbbp a strong band is found around 1483 and 1278 cm^{−1} attributed to $\nu_{C=N}$ and ν_{C-N} of the benzimidazole group, which becomes a medium band around 1473 and 1263 cm^{−1} for the Cd(II) complex. The shifts of the characteristic absorption bands imply that all four imine nitrogen atoms are coordinated to the cation center.

The electronic spectra of free mbbp, picric acid and the Cd(II) complex were recorded at 298 K in DMF solution. The ligand mbbp shows two strong absorption bands at 306 and 388 nm attributed to $\pi \rightarrow \pi^*$ transitions. Picric acid shows four strong absorption bands at 272, 327, 365, and 419 nm attributed to $\pi \rightarrow \pi^*$ and $n \rightarrow \pi^*$ transitions, respectively [24,25]. The Cd(II) complex exhibits three strong absorption bands at 298, 363 and 398 nm attributed to $\pi \rightarrow \pi^*$ and $n \rightarrow \pi^*$ transitions, indicating that the ligand mbbp is coordinated to the metal center.

Molecular structure in the crystal

Selected bond lengths and bond angles of the complex [Cd(mbbp)₂](pic)₂ are listed in Table 2.

Table 2. Selected bond lengths (Å) and bond angles (deg) for the Cd(II) complex^a.

Cd(1)–N(4)	2.2897(13)	Cd(1)–N(1) ^{#1}	2.3363(14)
Cd(1)–N(4) ^{#1}	2.2897(13)	Cd(1)–N(2)	2.3790(13)
Cd(1)–N(1)	2.3363(14)	Cd(1)–N(2) ^{#1}	2.3790(13)
N(4)–Cd(1)–N(4) ^{#1}	102.00(6)	N(1) ^{#1} –Cd(1)–N(2)	90.17(4)
N(4)–Cd(1)–N(1) ^{#1}	132.06(5)	N(1)–Cd(1)–N(2)	69.36(4)
N(4) ^{#1} –Cd(1)–N(1) ^{#1}	71.24(5)	N(4)–Cd(1)–N(2) ^{#1}	93.16(5)
N(4)–Cd(1)–N(1)	71.24(5)	N(4) ^{#1} –Cd(1)–N(2) ^{#1}	137.70(5)
N(4) ^{#1} –Cd(1)–N(1)	132.06(4)	N(1) ^{#1} –Cd(1)–N(2) ^{#1}	69.36(4)
N(1) ^{#1} –Cd(1)–N(1)	147.87(6)	N(1)–Cd(1)–N(2) ^{#1}	90.17(4)
N(4)–Cd(1)–N(2)	137.70(5)	N(2)–Cd(1)–N(2) ^{#1}	101.69(6)
N(4) ^{#1} –Cd(1)–N(2)	93.16(5)		

^a Symmetry transformation used to generate equivalent atoms: ^{#1} −*x*, *y*, −*z* + 1/2.

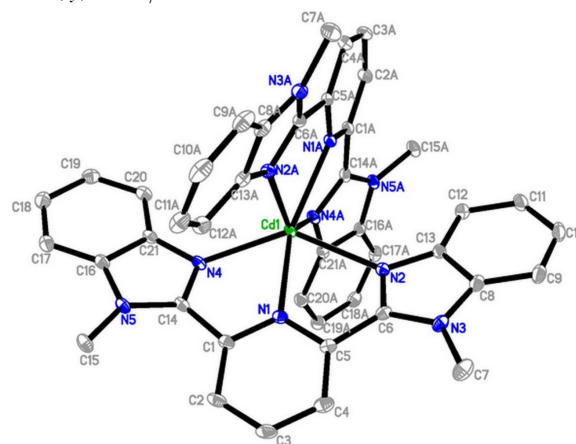


Fig. 1 (color online). Molecular structure of the [Cd(mbbp)₂]²⁺ cation with displacement ellipsoids drawn at the 30 % probability level; H atoms are omitted for clarity.

The structure consists of a [Cd(mbbp)₂]²⁺ cation (Fig. 1), and two picrate anions. The metal atom is six-coordinated with an N₆ ligand set of which four N atoms (N2, N4, N2A, N4A) are afforded by the benzimidazole rings and the other two (N1, N1A) by the pyridine rings. The shortest Cd–N bond length is 2.2897(13) Å [Cd(1)–N(4) or Cd(1)–N(4A)] and the longest is 2.3790(13) Å [Cd(1)–N(2) or Cd(1)–N(2A)]. The bond angles of ideal 90° are in the range from 71.24(5)° [N(4)–Cd(1)–N(1)] to 132.06(5)° [N(4)–Cd(1)–N(1A)], and of the ideal 180° from 102.00(6)° [N(4)–Cd(1)–N(4A)] to 147.87(6)° [N(1A)–Cd(1)–N(1)]. The coordination geometry of the Cd(II) center may be best described as distorted octahedral with N1, N2, N4, N1A from an equatorial plane. In the four selected nitrogen atoms, the maximum deviation distance (N1) from the least squares plane calculated for the four N atoms

is 0.383 Å, which indicates four selected coordinating nitrogen atoms almost in a plane. The bond angle of the two atoms (N2A, N4A) in axial positions is 137.70°, with distances from the plane of 2.120 and 2.195 Å, respectively. Therefore, compared with a regular octahedron, the data reflect a relatively distorted coordination octahedron [26–28].

DNA-binding properties

Absorption spectroscopic studies

The application of electronic absorption spectra in DNA-binding studies is one of the most useful tech-

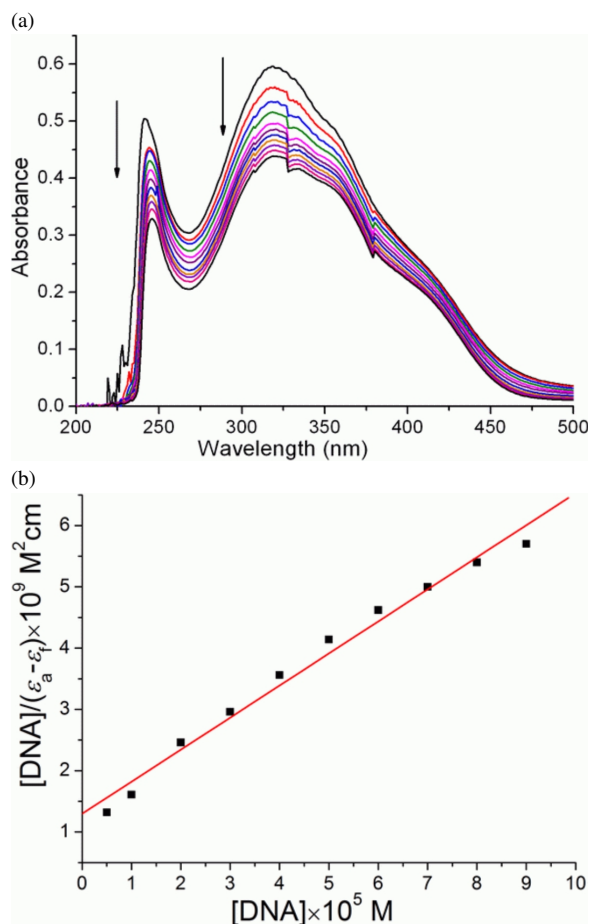


Fig. 2 (color online). (a) Electronic spectra of the Cd(II) complex (1.0×10^{-5} M) and in the presence of 0, 5, 10, 20, 30, 40, 50, 60, 70, 80, and 90 μL 2.5×10^{-3} M CT-DNA. The arrow shows the absorbance changes upon increasing CT-DNA concentration. (b) Plot of $[\text{DNA}]/(\epsilon_a - \epsilon_f)$ vs. $[\text{DNA}]$ for the titration of the Cd(II) complex with CT-DNA; ■, experimental data points; solid line, linear fitting of the data.

niques. The binding of intercalative drugs to DNA has been characterized classically through absorption titrations, following the hypochromism and red shift associated with binding of the colored complex to the helix [29]. The absorption spectra of the Cd(II) complex in the absence and presence of CT-DNA (at a constant concentration of complexes) are given in Fig. 2a. As can be seen from Fig. 2a, the Cd(II) complex exhibits an intense absorption band at 319 nm assigned to $\pi \rightarrow \pi^*$ transitions of the benzimidazole and picrate groups. Addition of increasing amounts of CT-DNA results in hypochromism in the UV/Vis spectra of the Cd(II) complex. In the present case, with addition of DNA, the Cd(II) complex exhibits hypochromism of about 26.6 % and bathochromism of 4 nm. These spectral characteristics suggest that the Cd(II) complex interacts with DNA, most likely through a mode that involves a stacking interaction between the aromatic chromophore and the base pairs [30, 31].

In order to further illustrate the binding strength of the Cd(II) complex, the intrinsic binding constant K_b was determined from the spectral titration data using the following equation [17]:

$$[\text{DNA}]/(\epsilon_a - \epsilon_f) = [\text{DNA}]/(\epsilon_b - \epsilon_f) + 1/K_b(\epsilon_b - \epsilon_f)$$

where $[\text{DNA}]$ is the concentration of DNA in base pairs, the apparent absorption coefficients ϵ_a , ϵ_f and ϵ_b correspond to $A_{\text{obsd}}/[\text{M}]$, the extinction coefficient of the free compound and the extinction coefficient of the compound when fully bound to DNA, respectively. In plots of $[\text{DNA}]/(\epsilon_a - \epsilon_f)$ vs. $[\text{DNA}]$, K_b is given by the ratio of the slope to the intercept. From the $[\text{DNA}]/(\epsilon_a - \epsilon_f)$ vs. $[\text{DNA}]$ plot (Fig. 2b), the binding constant K_b for the Cd(II) complex was estimated to be $4.03 \times 10^4 \text{ M}^{-1}$ ($R = 0.9922$ for ten points).

Fluorescence spectroscopic studies

In order to further study the binding properties of the complex with DNA, competitive binding experiments were carried out. The relative binding of the Cd(II) complex to CT-DNA was studied by the fluorescence spectral method using a solution of ethidium bromide (EB) bound CT-DNA in Tris-HCl/NaCl buffer (pH = 7.2). Ethidium bromide (EB) is a weakly fluorescent compound, but in the presence of DNA its emission intensity is greatly enhanced because of its strong intercalation between the adjacent DNA base pairs. It was

previously reported that the enhanced luminescence can be quenched by adding a second molecule [32, 33].

A competitive binding of the Cd(II) complex to CT-DNA resulted in the displacement of bound EB or in quenching of the bound EB, and as a consequence the emission intensity of ethidium bromide decreased. In the competitive binding experiment, a 10 μ L of CT-DNA solution was added to a 10 μ L of an EB buffer solution (pH = 7.2), and the fluorescence intensity was measured using the excitation wavelength of 520 nm resulting in an emission at about 600 nm at r. t.

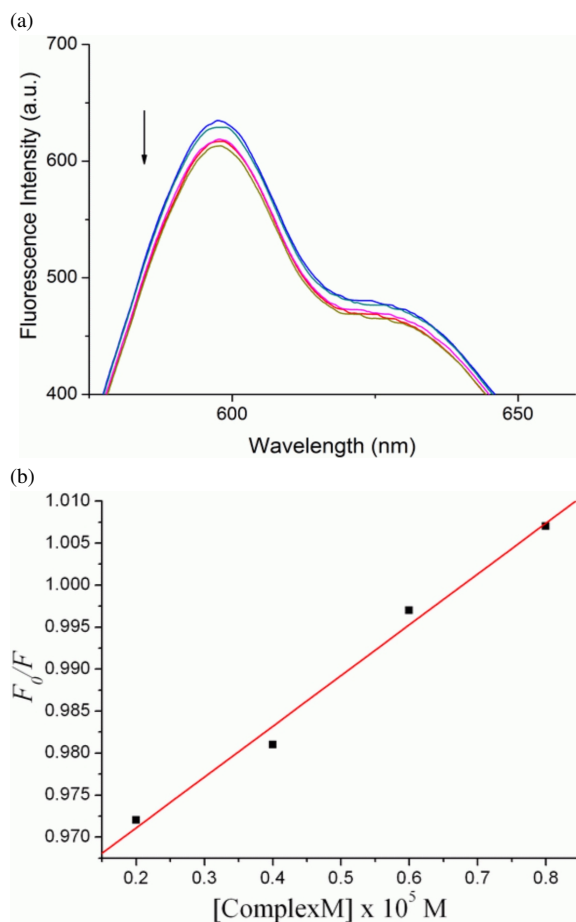


Fig. 3 (color online). (a) Fluorescence spectra of the binding of EB to DNA in the absence and presence of increasing amounts of the Cd(II) complex, $\lambda_{\text{ex}} = 520$ nm, [EB] = 8.8×10^{-6} M, [CT-DNA] = 1×10^{-5} M. The arrow shows the absorbance changes upon increasing CT-DNA concentration. (b) Stern-Volmer quenching plot of F_0/F vs. [Complex] for the titration of EB bound to CT-DNA by the Cd(II) complex; ■, experimental data points; solid line, linear fitting of the data.

Upon addition of the Cd(II) complex, the emission intensity of EB-bound calf thymus (CT-DNA) solution decreases, indicating that the complex competes with EB to bind with DNA (Fig. 3a). The extent of reduction of the emission intensity gives a measure of the binding propensity of the complex to CT-DNA. According to the classical Stern-Volmer equation [32, 34]:

$$F_0/F = 1 + K_{\text{sv}} [Q]$$

where F_0 is the emission intensity in the absence of the quencher, F is the emission intensity in the presence of the quencher, K_{sv} is the quenching constant and $[Q]$ is the Cd(II) complex. The fluorescence quenching constant (K_{sv}) of the Cd(II) complex (Fig. 3b) is $6.05 \times 10^3 \text{ M}^{-1}$ ($R = 0.9941$ for four points). K_{sv} is a linear Stern-Volmer quenching constant dependent on the ratio of the bound concentration of EB to the concentration of DNA. It may be due to the Cd(II) complex interacting with DNA in partial intercalation mode, so releasing some free EB from the EB-bound CT-DNA complex system, which is consistent with the above absorption spectral result.

Viscosity studies

Optical photophysical techniques are widely used to study the binding model of a ligand and its metal complexes with DNA, but give no sufficient clues to support a binding model. Therefore, viscosity measurements were carried out to further clarify the interaction of the metal complex and DNA. Hydrodynamic

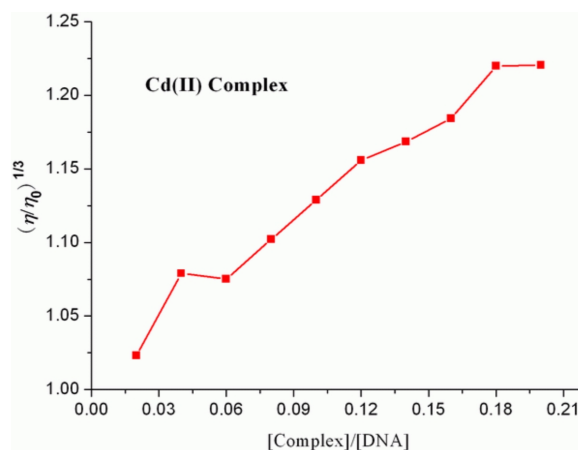


Fig. 4 (color online). Effects of increasing amounts of $[\text{Cd}(\text{mbbp})_2]^{2+}$ (■) on the relative viscosity of CT-DNA at 25 ± 0.1 °C; [DNA] = 5×10^{-5} M.

measurements that are sensitive to the length change (*i. e.*, viscosity and sedimentation) are regarded as the least ambiguous and the most critical tests of a binding model in solution in the absence of crystal structure data [35, 36]. With increasing amounts of the title Cd(II) complex, the viscosity of DNA increases steadily. The values of $(\eta - \eta_0)^{1/3}$ were plotted against [complex]/[DNA] (Fig. 4). In classical intercalation, the DNA helix lengthens as base pairs are separated to accommodate the bound ligand leading to increased DNA viscosity, whereas a partial, non-classical ligand intercalation causes a bend (or kink) in the DNA helix reducing its effective length and thereby its viscosity [36].

The effects of the Cd(II) complex on the viscosity of CT-DNA are shown in Fig. 4. The viscosity of CT-DNA is increased steadily with the increment of the Cd(II) complex, and it is further illustrated that the Cd(II) complex intercalates with CT-DNA [36]. The result of the viscosity experiments confirms the mode of the Cd(II) complex intercalation into DNA

base pairs already established through absorption and fluorescence spectroscopic studies.

Conclusion

In summary, a novel Cd(II) picrate complex based on the V-shaped ligand mbbp has been synthesized and characterized. The interaction of the Cd(II) complex with CT-DNA was explored by using absorption and fluorescence spectral techniques and viscosity measurements. The data suggest that the Cd(II) complex binds to CT-DNA in an intercalation mode, and this result can be helpful for the design of drugs and pharmaceuticals on a molecular level and warrant further *in vivo* experiments and pharmacological assays.

Acknowledgement

The authors acknowledge the financial support and a grant from 'Qing Lan' Talent Engineering Funds by Lanzhou Jiaotong University. The grant from the Middle-Young Age Science Foundation (grant no. 3YS061-A25-023) and 'Long Yuan Qing Nian' of Gansu Province is also acknowledged.

- [1] J. K. Barton, *Science* **1986**, 233, 727–734.
- [2] K. E. Erkkila, D. T. Odom, J. K. Barton, *Chem. Rev.* **1999**, 99, 2777–2795.
- [3] L. N. Ji, X. H. Zou, J. G. Lin, *Coord. Chem. Rev.* **2001**, 216–217, 513–536.
- [4] B. M. Zeglis, V. C. Pierre, J. K. Barton, *Chem. Commun.* **2007**, 4565–4579.
- [5] J. V. Higdon, E. Ho, *Metallotherapeutic Drugs and Metal-Based Diagnostic Agents: The Use of Metals in Medicine*. John Wiley, Chichester, **2005**.
- [6] V. G. Vaidyanathan, B. U. Nair, *J. Inorg. Biochem.* **2002**, 91, 405–412.
- [7] V. G. Vaidyanathan, B. U. Nair, *J. Inorg. Biochem.* **2003**, 93, 271–276.
- [8] V. G. Vaidyanathan, B. U. Nair, *J. Inorg. Biochem.* **2003**, 94, 121–126.
- [9] V. G. Vaidyanathan, B. U. Nair, *Eur. J. Inorg. Chem.* **2003**, 3633–3638.
- [10] J. L. Wang, L. Shuai, X. M. Xiao, Y. Zeng, Z. L. Li, M.-I. Takeko, *J. Inorg. Biochem.* **2005**, 99, 883–885.
- [11] N. M. Aghatabay, A. Neshat, T. Karabiyik, M. Somer, D. Hacı, B. Dülger, *Eur. J. Med. Chem.* **2007**, 42, 205–213.
- [12] H. L. Wu, X. C. Huang, J. K. Yuan, F. Kou, F. Jia, B. Liu, K. T. Wang, *Eur. J. Med. Chem.* **2010**, 45, 5324–5330.
- [13] H. L. Wu, X. C. Huang, J. K. Yuan, F. Kou, G. S. Chen, B. B. Jia, Y. Yang, Y. L. Lai, *Z. Naturforsch.* **2010**, 65b, 1334–1340.
- [14] J. Marmur, *J. Mol. Biol.* **1961**, 3, 208–218.
- [15] M. F. Reichmann, S. A. Rice, C. A. Thomas, P. Doty, *J. Am. Chem. Soc.* **1954**, 76, 3047–3053.
- [16] T. B. Chaires, N. Dattagupta, D. M. Crothers, *Biochem.* **1982**, 21, 3933–3940.
- [17] A. Wolf, G. H. Shimer, Jr., T. Meehan, *Biochem.* **1987**, 26, 6392–6396.
- [18] A. W. Addison, P. J. Burke, *J. Heterocycl. Chem.* **1981**, 18, 803–805.
- [19] RAPID-AUTO, Rigaku/MS, The Woodlands, Texas (USA), **2004**.
- [20] G. M. Sheldrick, SHELXTL, Siemens Analytical X-Ray Instruments, Inc., Madison, Wisconsin (USA) **1996**. See also: G. M. Sheldrick, *Acta Crystallogr.* **1990**, A46, 467–473; *ibid.* **2008**, A64, 112–122.
- [21] W. J. Geary, *Coord. Chem. Rev.* **1971**, 7, 81–122.
- [22] C. Piguet, B. Bocquet, E. Muler, A. F. Williams, *Helv. Chim. Acta* **1989**, 72, 323–337.
- [23] W. J. Zhang, W. H. Sun, S. Zhang, J. X. Hou, K. Wedeking, S. Schultz, R. Fröhlich, H. B. Song, *Organometallics* **2006**, 25, 1961–1969.
- [24] H. L. Wu, R. R. Yun, K. T. Wang, K. Li, X. C. Huang, T. Sun, *Z. Anorg. Allg. Chem.* **2010**, 636, 629–633.
- [25] H. L. Wu, R. R. Yun, K. T. Wang, K. Li, X. C. Huang, T. Sun, Y. Y. Wang, *Z. Anorg. Allg. Chem.* **2010**, 636, 1397–1400.
- [26] N. Yoshikawa, S. Yamabe, N. Kanehisa, Y. Kai, H. Takashima, K. Tsukahara, *Eur. J. Inorg. Chem.* **2007**, 1911–1919.

- [27] D. Kang, J. Seo, S. Y. Lee, J. Y. Lee, K. S. Choi, S. S. Lee, *Inorg. Chem. Commun.* **2007**, *10*, 1425–1428.
- [28] J. P. Collin, I. M. Dixon, J. P. Sauvage, J. A. G. Williams, F. Barigelletti, L. Flamigni, *J. Am. Chem. Soc.* **1999**, *121*, 5009–5016.
- [29] A. M. Pyle, J. P. Rehmann, R. Meshoyrer, C. V. Kumar, N. J. Turro, J. K. Barton, *J. Am. Chem. Soc.* **1989**, *111*, 3051–3058.
- [30] J. K. Barton, A. T. Danishefsky, J. M. Goldberg, *J. Am. Chem. Soc.* **1984**, *106*, 2172–2176.
- [31] S. A. Tysoc, R. J. Morgan, A. D. Baker, T. C. Streckas, *J. Phys. Chem.* **1993**, *97*, 1707–1711.
- [32] J. R. Lakowicz, G. Webber, *Biochem.* **1973**, *12*, 4161–4170.
- [33] B. C. Baguley, M. LeBret, *Biochem.* **1984**, *23*, 937–943.
- [34] M. R. Efink, C. A. Ghiron, *Anal. Biochem.* **1981**, *114*, 199–206.
- [35] S. Satyanarayana, J. C. Dabroniak, J. B. Chaires, *Biochem.* **1992**, *31*, 9319–9324.
- [36] S. Satyanarayana, J. C. Daborusak, J. B. Chaires, *Biochem.* **1993**, *32*, 2573–2584.